JOURNAL OF STRUCTURAL BIOLOGY 112, 3–10 (1994)

Native Talin Is a Dumbbell-Shaped Homodimer When It Interacts with Actin

WOLFGANG H. GOLDMANN,* ANDREAS BREMER,†,[1] MARKUS HÄNER,† UELI AEBI,† AND GERHARD ISENBERG*,[2]

*Department of Biophysics, E22, Technical University of Munich, D-85747 Garching, Federal Republic of Germany; and †M. E. Müller-Institute, Biozentrum, University of Basel, CH-4056 Basel, Switzerland

Received January 21, 1994, and in revised form January 31, 1994

Electron microscopy of glycerol-sprayed and rotary metal-shadowed talin from human platelets reveals a dumbbell-shaped molecule with an average length of ~51 nm. Analytical ultracentrifugation of native talin yields a single molecular species with an apparent molecular mass of 412 (±28.6) kDa and a sedimentation coefficient of s_{20w} = 11.2. Chemical cross-linking with glutaraldehyde (GA) and corresponding SDS–PAGE analysis show that the monomer band of talin can be quantitatively converted to a dimer band at GA concentrations ≥0.45%, indicating that there is no significant amount of monomer present in solution. These structural and biophysical data are compatible with native talin being an antiparallel homodimer. Length measurements and viscometric and fluorescent assays of actin filaments polymerized in the presence of native talin and of covalently cross-linked talin dimers all yield similar effects: namely, increased nucleation and polymerization rates and an overall reduction of actin filament length. Hence, we conclude that talin in its native biological state is a dimer when promoting nucleation of actin filaments.

INTRODUCTION

Anchorage and nucleation of actin filament formation at the plasma membrane is a prerequisite for the protrusion of the leading edge in moving cells. In search of proteins which could trigger these events, we have been successful in identifying talin, a major constituent of focal contacts (Burridge and Connell, 1983) and guiding cell lamellipodia (DePasquale and Izzard, 1991), as a potential missing link (Isenberg and Goldmann, 1992, 1994). Talin is an actin (Muguruma *et al.*, 1990; Goldmann and Isenberg, 1991) and lipid binding protein (Heise *et al.*, 1991; Isenberg, 1991; Goldmann *et al.*, 1992). It inserts into the hydrophobic domain of lipid mono- and bilayers (Dietrich *et al.*, 1993; Goldmann *et al.*, 1992). Most exciting, we found that talin promotes actin filament formation *in vitro* by facilitating actin filament nucleation leading to a rapid increase of filament number concentration over filament length (Kaufmann *et al.*, 1992). Viscoelastic measurements have revealed that actin filaments formed in the presence of talin also exhibit an increased internal stiffness (Ruddies *et al.*, 1993), a property which is compatible with the hypothesis that the unidirectional polymerization of actin filaments at the leading edge of moving cells (Small *et al.*, 1978) may be utilized for vectorial force production (cf. Isenberg *et al.*, 1978).

As demonstrated by direct observation using high intensity fluorescent light microscopy, talin, when reconstituted into lipid vesicle membranes, nucleates actin filament growth directly at the membrane interface, a behavior comparable to its function in solution (Kaufmann *et al.*, 1991, 1992).

Thus far, only limited data exist on the molecular architecture of native talin. From its primary sequence, which consists of 2541 amino acids, the molecular mass of the polypeptide was determined to be 269.854 Da (Rees *et al.*, 1990). A cleavage site between residues 433 and 434 yields a N-terminal head region of 49.981 Da and a long C-terminal tail domain of 219.873 Da. The head piece, which exhibits a high degree of homology with the membrane binding proteins 4.1 and ezrin, indeed harbors a lipid binding site (Niggli *et al.*, 1994), whereas the C-terminal tail region carries binding sites for vinculin (Gilmore *et al.*, 1993) and integrin (Horwitz *et al.*, 1986).

The intact talin molecule yields a high content of α-helices (70–80%) (Molony *et al.*, 1987). Fourier-transformed computer analysis of its primary sequence has revealed a set of repetitive α-helical motifs (McLachlan *et al.*, 1994), suggesting a rod-like

[1] Present address: Department of Cell Biology, Duke University Medical Center, Durham, NC 27704.

[2] To whom correspondence should be addressed at Technical University of Munich, Department of Biophysics, E22, James Franck Strasse, D-85748 Garching, FRG. Fax: 49(89)-3209 2469.

1047-8477/94 $6.00

structure comparable to those of spectrin, α-actinin, and dystrophin (Cross *et al.*, 1990; Dhermy, 1991). In analogy to these antiparallel homodimers, it was speculated that the active form of talin might also be a dimer of two antiparallel, closely associated chains coupled into repetitive motifs of antiparallel coiled-coil structure (McLachlan *et al.*, 1994).

Here we present electron microscopic data of the talin molecule which are consistent with the suggestion that talin forms antiparallel dumbbell-shaped homodimers. Moreover, we provide evidence from analytical ultracentrifugation studies that the major species of native talin molecules behave as a dimer. Finally, covalently cross-linked talin dimers effectively nucleate actin filament polymerization.

MATERIALS AND METHODS

Reagents

NBD (7-chloro-4-nitrobenz-2-oxa-1,3-diazole) was purchased from Sigma (Deisenhofen, FRG); EDC [1-ethyl-3-3(3-dimethylaminopropyl)carbodiimide hydrochloride] was acquired from Pierce (Rockford, IL); GA (glutaraldehyde) was bought from Electron Microscopy Sciences (Forth Washington, PA); 1,2-PBM (*N,N'*-1,2-phenylenebismaleimide) was obtained from Aldrich Chemical Co. (Milwaukee, WI).

Proteins

Platelet talin was isolated from outdated human thrombocytes as described by Kaufmann *et al.* (1991). The protein was purified to homogeneity as judged by SDS–PAGE (see Fig. 4), and the protein concentration was determined by the method of Bradford (1976).

Actin was prepared by the method of Spudich and Watt (1971) from an acetone powder obtained from rabbit back muscles followed by a gel filtration step as described by MacLean-Fletcher and Pollard (1980). The G-actin peak fractions at ~1–2 mg/ml were stored in G-buffer (2 m*M* Tris/HCl, pH 7.5, 0.2 m*M* $CaCl_2$, 0.2 m*M* DTT, 0.5 m*M* ATP) at 4°C.

Electron Microscopy

For glycerol spraying /low-angle rotary metal shadowing, a 20-μl aliquot of talin (final concentration: 0.1–0.3 mg/ml in 30% glyercol) was sprayed onto a piece of freshly cleaved mica. The mica piece was placed *en face* on the rotary table of a BA 511 M freeze-etch apparatus (Balzers AG., F1-9496 Balzers, Fürstentum Liechtenstein) and dried *in vacuo* at room temperature for at least 1 hr. Finally, the dried sample was rotary-shadowed with platinum/carbon at an elevation angle of 3–5° (Fowler and Aebi, 1983). Molecular length distributions were plotted as histograms and fitted by single Gaussian curves, using the Marquardt algorithm described by Bevington (1969).

The length distribution of actin filaments polymerized in the presence of talin was evaluated on negatively stained actin filaments which were polymerized in the presence of talin at a molar ratio of 4:1. For this purpose, a 5-μl aliquot of the sample was adsorbed for 1 min to a glow-discharged (Aebi and Pollard, 1987), carbon-coated collodion film on a copper grid. Then the grid was washed on one drop of either distilled water or buffer before it was sequentially placed on three drops of 0.75% uranyl formate (pH 4.25) for ~10 sec each. Excess liquid was drained with filter paper followed by suction with a capillary along the edge of the grid which was then permitted to air dry.

Specimens were examined in a Hitachi H-7000 transmission electron microscope operated at 100 kV. Electron micrographs were recorded on Kodak SO-163 electron image film at nominal magnifications of either × 20 000 or × 50 000. Magnification calibration was performed according to Wrigley (1968) using negatively stained catalase crystals.

Analytical Ultracentrifugation

Both sedimentation velocity and sedimentation equilibrium measurements were performed in a Beckman model Optima XL-A analytical ultracentrifuge (Beckman Instruments Co., Fullerton, CA). Sedimentation velocity runs were carried out at 56 000 rpm and 12°C using an Epon 12-mm double-sector cell. Photoelectric scans were recorded at wavelengths of 230 and 280 nm.

For sedimentation equilibrium runs the same cell type was used but only filled up to 3 mm column height. To evaluate the different M_r species contained in multicomponent solutions, two rotor speeds, i.e., 5 200 and 6 800 rpm were used (Chernyak and Magretova, 1982). To calculate M_r, a program that adjusts the baseline absorbance such as to obtain the best linear fit of ln *A* vs. r^2 (written by H. Berger and A. Lustig, Biocenter, Basel) was used. For all calculations a partial specific volume (υ) of 0.73 ml/g was used.

Covalent Cross-Linking

A 30-μl aliquot of talin (0.9 mg/ml) was diluted with an equal volume of buffer (Buffer T: 50 m*M* Tris/HCl, pH 8.0, 3 m*M* EDTA, 0.1 m*M* DDT). Five-microliter aliquots were cross-linked with an equal volume of GA at rising concentrations (0.01–0.8% prepared from an 8% stock solution in Buffer T) for 2 min on ice. The reaction was stopped by adding 10 μl glycine (2% final concentration in Buffer T). For molecular weight analysis samples were applied to 3–15% gradient SDS–PAGE gels (Laemmli, 1970).

Functional Assays of GA-Cross-Linked Talin Dimers

Talin (0.78 mg/ml) was quantitatively and covalently cross-linked into dimers with ≥0.45% GA as described above. The reaction was stopped with 2% glycine. Chemically cross-linked talin dimers were dialyzed overnight against Buffer T and subsequently used to nucleate actin polymerization which was assayed by fluorescence increase of NBD-labeled (5%) actin solutions and by falling ball viscometry (Kaufmann *et al.*, 1991).

RESULTS

Molecular structure

Electron microscopy of glycerol-sprayed/rotary metal-shadowed purified talin revealed dumbbell-shaped molecules with a globular head at both ends and with indications of a hinge in the middle of the rod most likely representing antiparallel homodimers of talin (Figs 1a and 1b). This molecular architecture is deduced from the fact that besides some easily recognizable fragments (cf. Fig. 1a), these rods represented the only molecular species in our preparations which, by analytical ultracentrifugation of the same samples (cf. below), were clearly identified as talin dimers. Length measurements of 184 individual molecules were put into a histogram which was fitted with a single Gaussian curve to yield an average molecular length of 51 (±2.4) nm (Fig. 1c). These dimensions as well as the dumbbell-like shape of the molecule agree with predictions based on a detailed sequence analysis of the polypeptide (McLachlan *et al.*, 1994). Interruptions in

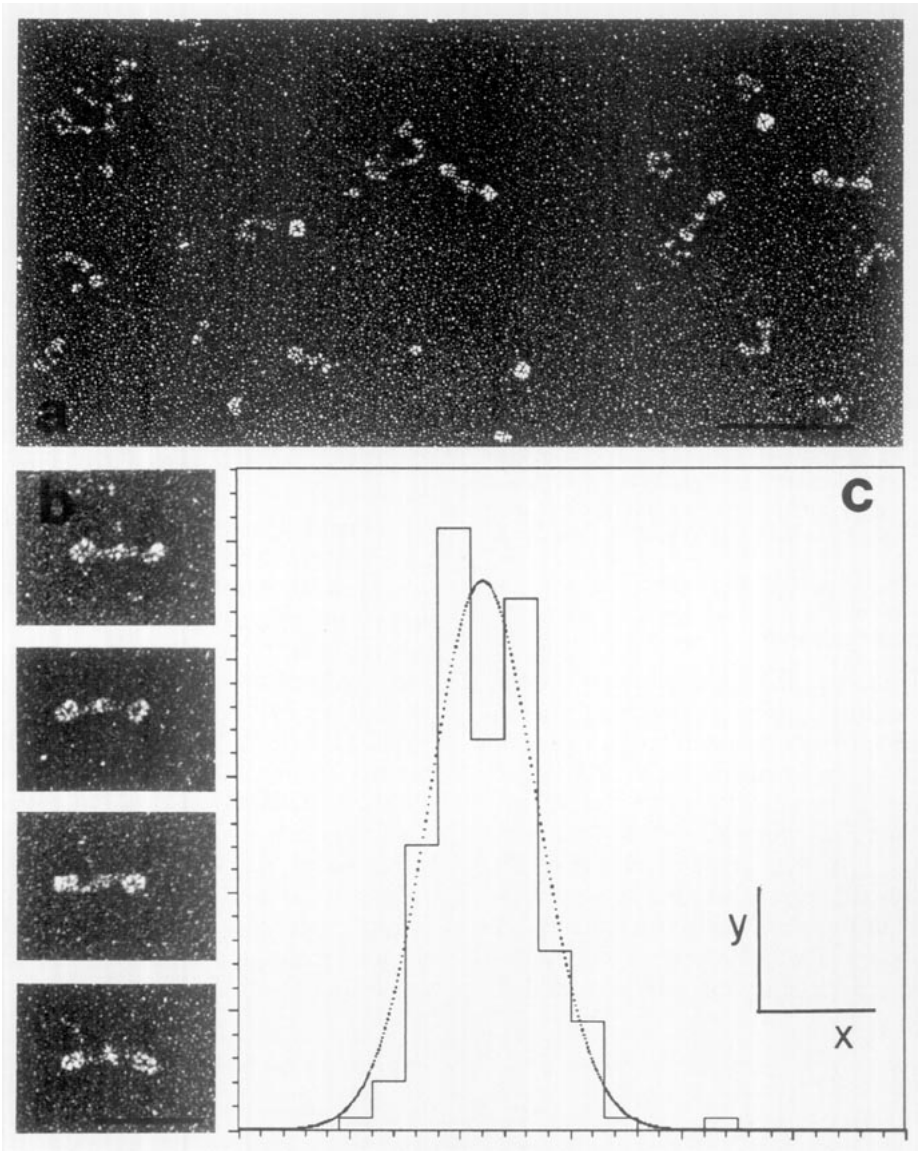

FIG. 1. Electron microscopy of glycerol-sprayed, rotary metal-shadowed talin in 50 m*M* Tris/HCl, 2 m*M* EDTA, 0.1 m*M* DTT, pH 8, at a final concentration of 0.1–0.3 mg/ml (in 30% glycerol). (a) Low magnification overview and (b) gallery of selected talin molecules; scale bars, 100 nm (a) and 50 nm (b). (c) The lengths of 184 talin molecules such as shown in (b) have been measured and put into a histogram which has been fitted with a single Gaussian curve. The average length of the measured molecules amounts to 51 (SD ± 2.4) nm. The origin of the *x*-axis is at 40 nm and its scale is 5 nm, whereas the *y*-axis starts at 0 with a scale of 10 filaments.

the regular sequence pattern of the tail domain may give rise to a region of greater flexibility as indicated by a hinge region in the middle of the talin dimer (cf. Fig. 1b).

Effect of Talin on Actin Filament Length

It has previously been documented by four independent methods (Kaufmann *et al.*, 1991, 1992; Ruddies *et al.*, 1993), i.e., dynamic light scattering, fluorescence recovery after photobleaching, high resolution fluorescent light microscopy, and rheological measurements that talin is able to nucleate the rapid formation of actin filaments leading to an increase of filament number concentration over filament length during the early time course of actin polymerization. Quantitative length measurements of negatively stained actin filaments polymerized in the absence/presence of talin (Fig. 2) support the notion that the filament length is considerably reduced (to ~1 μm) on the time scale between 0 and 10 min in the presence of a talin to actin molar ratio of 1:4. With progressing time, this difference becomes less pronounced and eventually insignificant at steady state, since slowly but definitely the short filaments anneal into long polymer chains, a behavior which agrees with the description of the viscoelastic properties of talin-induced actin networks (Ruddies *et al.*, 1993).

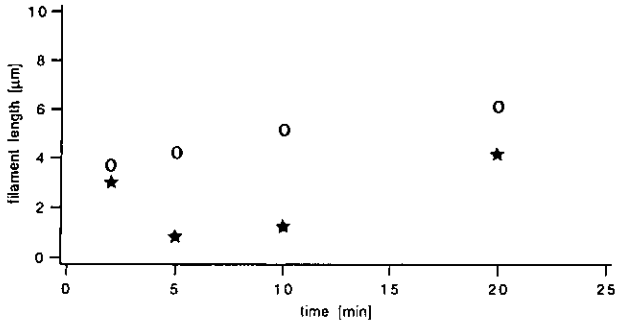

FIG. 2. Time-dependent effect of talin on the length of polymerizing actin filaments. For each time point the contour length of an average of 25 filaments each polymerized in the absence (open circles) and in the presence (filled stars) of talin were measured. For this purpose, G-actin at 1 mg/ml, equilibrated in 2 m*M* Tris/HCl, 0.2 m*M* $CaCl_2$, 0.2 m*M* DTT, 0.5 m*M* ATP, pH 7.5, was mixed with talin at a molar ratio of 4/1 (actin/talin) and immediately polymerized by adding KCl to 100 m*M* and $MgCl_2$ to 2 m*M*.

Analytical Ultracentrifugation

Figures 3a and 3b reveal representative photoelectric scans of sedimentation velocity and sedimentation equilibrium runs performed with native platelet talin in a Beckman Optima XL-A analytical ultracentrifuge. For determination of the sedimentation coefficient, samples were run at 48 000 rpm and 12°C. The OD_{280nm} of the sample during the run shown in Fig. 3a was 0.1, corresponding to a protein concentration of 0.286 mg/ml, using an extinction coefficient of $E_{280,\ 1\%} = 3.49$ (Molony *et al.*, 1987). With $\upsilon = 0.73$ ml/g, $\rho = 1.013$ g/ml, and $\mu = 1.06$, a sedimentation coefficient of $s_{20w} = 11.2$ was calculated.

Sedimentation equilibrium analysis at 5 200 and 6 800 rpm (Fig. 3b) yielded a linear relationship in ln A_{280} versus r^2 plots (Fig. 3b; inset). From such linear regressions an average molecular mass of ~412 kDa was deduced (see Table 1). Knowing the molecular mass of talin monomers, which based on its primary sequence equals 269.854, our data are most consistent with native talin being predominantly a dimer.

Covalent Cross-Linking

Among various protein cross-linking reagents: (EDC, 1,2-PBM, and GA) GA was found to be the most effective reagent for covalent intersubunit cross-linking of native talin. By SDS–PAGE unreacted talin yields an apparent M_r of ~215 kDa (Fig. 4A, lane 2). After reaction of native talin with increasing concentrations of GA (0.01–0.8%) (Fig. 4A, lanes 2–13) the monomer band is gradually attenuated concomitant with the appearance of a gradually increasing band corresponding to an apparent M_r of ~417 kDa (cf. Fig. 4A, lanes 7–13), which approximately doubles the apparent denatured molecular mass of ~215 kDa. At a GA concentration ≥0.2% the monomer band is quantitatively shifted to a dimer band. At GA concentrations ≥0.5% (Fig. 4A, lane 10) a second type of dimer appears with an apparent molecular mass of ~509 kDa as judged from the molecular mass plot displayed in Fig. 4B. The most likely explanation for this behavior is that

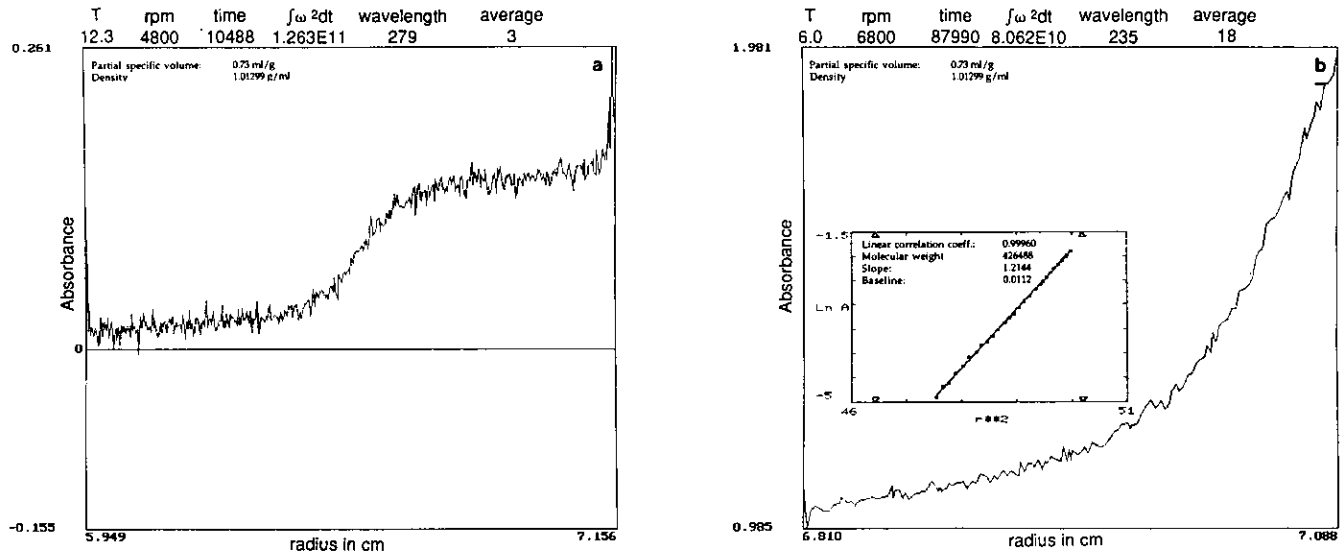

FIG. 3. Sedimentation velocity and sedimentation equilibrium analysis of talin equilibrated in 50 m*M* Tris/HCl, 2 m*M* EDTA, 0.1 m*M* DTT, pH 8. (a) For sedimentation velocity, talin at 0.1–0.3 mg/ml was placed in a 12-mm double-sector cell made of Epon and run at 48 000 rpm and 12°C. Photoelectric scans were recorded at wavelengths of 230 and 280 nm. (b) For sedimentation equilibrium runs, the same cell type was used but only filled up to 3 mm column height (i.e., ~0.11 ml per sector). All equilibrium runs were performed at 5 200 and 6 800 rpm, and the temperature was kept at 6°C. Upon reaching equilibrium, photoelectric scans were recorded at 230 and 280 nm. (Inset) Linear fit of ln *A* (concentration) plotted versus r^2 (radial distance in the cell).

TABLE I
Data from Various Sedimentation Velocity and Sedimentation Equilibrium Experiments

Talin in 50 m*M* Tris/HCl, 3 m*M* EDTA, 0.1 m*M* DTT, pH 8.0
$\text{Concentration}_{\text{talin,280nm}}$ = 0.286 mg/ml

(A) Sedimentation velocity:
Centrifugation at 48 000 rpm and 12°C
Sedimentation coefficient s_{20w} = 11.2 (±0.05) (n = 2)

(B) Sedimentation equilibrium:
Centrifugation at 6°C

5200 rpm		6800 rpm	
λ = 279 nm	417 kDa	λ = 279 nm	435 kDa
λ = 279 nm	430 kDa	λ = 279 nm	453 kDa
λ = 279 nm	419 kDa		
		λ = 235 nm	426 kDa
λ = 233 nm	367 kDa	λ = 233 nm	373 kDa
λ = 232 nm	380 kDa	λ = 232 nm	416 kDa

Molecular mass (M_r): 412 (±28.6) kDa; (n = 10)

Note. The sedimentation coefficient s_{20w} = 11.2 (±0.05) (n = 2) has been taken from Fig. 3a, and the molecular mass M_r 412 (±28.6) kDa (n = 10) has been taken from Fig. 3b. Numbers in parentheses are the standard deviation and the number of observations, respectively.

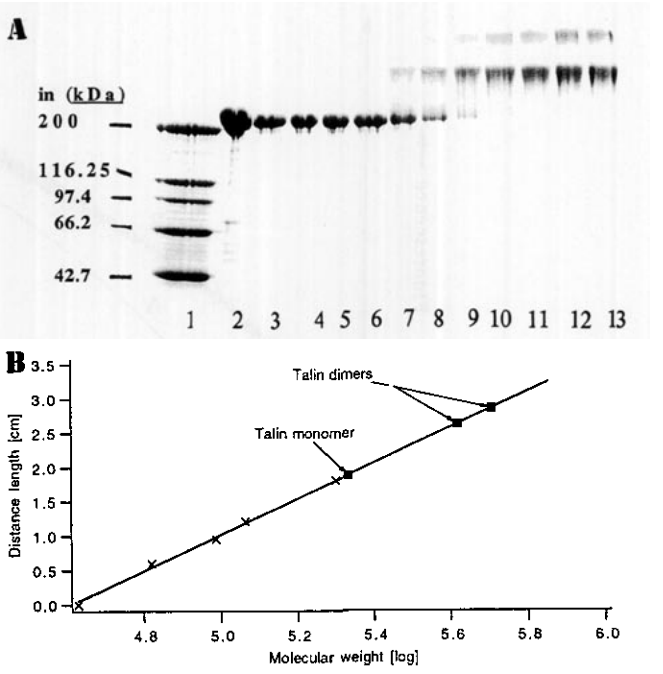

FIG. 4. Analysis of talin cross-linked with increasing amounts of GA by SDS–PAGE. (A) 3–15% gradient gel: lane 1, MW standards; lanes 2–13, the same amount of talin cross-linked with increasing amounts of GA: no GA (2), 0.01% (3), 0.02% (4), 0.05% (5), 0.1% (6), 0.2% (7), 0.3% (8), 0.4% (9), 0.5% (10), 0.6% (11), 0.7% (12), and 0.8% (13). Cross-linking of talin was performed as described under Materials and Methods. (B) Linear fit of the apparent mobilities of the MW standards as measured in (A) when plotted versus the log of their MW. On the fitted curve monomeric talin runs with an apparent MW of ~215 kDa, whereas the two cross-linked talin bands run with apparent mobilities of ~417 and ~509 kDa, respectively.

some dimer modification—possibly due to intermolecular cross-linking—has occurred which results in an anomalous mobility on SDS–PAGE. Alternatively, this band could represent a second type of cross-link of the dimer (Millonig *et al.*, 1988). As with sufficient cross-linker no monomer band is depicted by SDS–PAGE, we have to assume that no significant amount of monomer is present in solution.

Functional Assays with Cross-Linked Talin Dimers

We have chosen the lowest GA concentration (i.e., 0.45%, see Fig. 4A) necessary to quantitatively cross-link talin in its dimer configuration. After quenching with glycine and extensive dialysis (cf. Materials and Methods), the cross-linked talin dimer fraction was tested with respect to its capacity to nucleate actin polymerization and to reduce the viscosity of polymerizing actin solutions (cf. Kaufmann *et al.*, 1991; Goldmann *et al.*, 1992). As documented in Fig. 5, curve A, upon polymerization actin yields an increase in NBD fluorescence. When cross-linked talin dimers are added at a molar ratio of 1/2 (talin/actin) at the beginning of polymerization a distinct and significant nucleation effect is revealed (Fig. 5, curve B) which is comparable to our previous published data. Low-shear viscometry was performed on actin solutions which were polymerized for 30 min in the absence (control) and in the presence of native talin or cross-linked talin dimers at a molar talin/actin ratio of 1/2. Compared to F-actin alone (=100%), the polymerization of actin in the presence of native talin yields a reduction of the low-shear viscosity to 12% (Fig. 5, inset). Under identical conditions covalently cross-linked talin dimers yield a decrease of viscosity to 38% (Fig. 5, inset). The observation that cross-linked talin yields a smaller reduction of the low-shear viscosity of polymerized actin than native talin may result from chemical cross-linking and extensive dialysis after quenching with glycine, thus yielding a subtle denaturation of the modified talin.

Since the actin nucleating effect and the viscosity reducing capacity—due to an increase of filament number concentration over filament length—are maintained with covalently cross-linked talin dimers, we conclude that talin in its native, biologically active state operates as a dimer.

DISCUSSION

We have accumulated experimental evidence that talin from human platelets in its biologically active state is a dumbbell-shaped dimer. Electron microscopy of glycerol-sprayed, rotary metal-shadowed specimens reveals distinct rod-like molecules with a globular domain at each end being consistent with antiparallel association of two talin monomers each

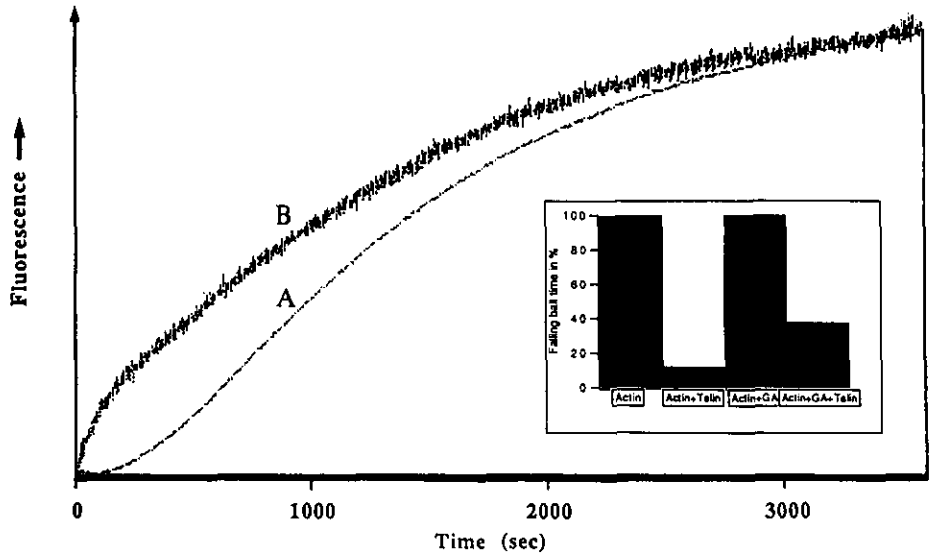

FIG. 5. Effect of GA-cross-linked talin dimers on actin polymerization. For control (curve A), 4.5 μM unmodified actin plus 0.5 μM NBD-labeled actin (= total of 5 μM actin) was polymerized in F-buffer (2 mM Tris/HCl, pH 7.5, 100 mM KCl, 2 mM $MgCl_2$, 0.2 mM $CaCl_2$, 0.2 mM DTT, 0.5 mM ATP). Curve B, 5 μM actin polymerized in the presence of 2.5 μM talin dimers cross-linked with 0.45% glutaraldehyde. The increase in fluorescence (arbitrary units) was measured as a function of time. (*Note:* The trace and the rate of actin polymerization in the *presence/absence* of 0.45% GA were similar). (Inset) Viscosity reducing activity of unmodified talin and cross-linked talin dimers in actin filament solutions. Actin was polymerized in the presence of unmodified talin (2:1 molar ratio) or of GA-cross-linked talin at the same concentration. Unmodified talin reduces the low-shear viscosity of F-actin to 12% and cross-linked talin dimers to 38%, compared to pure F-actin (= 100%). Glutaraldehyde (0.45%) alone had no effect on the low-shear viscosity of F-actin.

consisting of a globular head domain and a rod-like tail region. The molecular length of these talin dimers was measured to be 51 (±2.4) nm. This value is close to the 60-nm value reported by Molony *et al.* (1987). Moreover, this dumbbell-shaped antiparallel dimer configuration agrees with model predictions derived from computer-based Fourier sequence analysis, a method applied to detect periodic patterns of protein sequences (McLachlan *et al.*, 1994). As proposed by these authors, the talin sequence contains α-helical motifs which, because of their repeating nature, associate to form antiparallel arranged rods similar to other rod-like molecules, e.g., α-actinin, spectrin, and dystrophin (Cross *et al.*, 1990; Dhermy, 1991). Due to several proline residues along the sequence, the α-helical tail region is discontinuous, giving rise to loop formations (McLachlan *et al.*, 1994). Exactly, as documented in Fig. 1b, the talin dimer reveals a "knob" or "partially unraveled" region in the center of its rod, which might function as a flexible hinge. Indeed, glycerol-sprayed/rotary metal-shadowed talin preparations yielded a whole range of bent configurations including horseshoe-like molecules (data not shown). Since the rod domain is hydrophobic in nature (McLachlan *et al.*, 1994) the hinge region could also contribute to another lipid binding site.

By analytical ultracentrifugation, native talin preparations in low salt buffer at pH 8.0 contain predominantly a single species of molecules with an average M_r of 412 (±28.6) kDa and an average sedimentation coefficient s_{20w} = 11.2 (±0.05), indicating that talin exists in a dimer configuration rather than in a monomeric state (M_r 270 kDa in solution). Molony *et al.* (1987) have suggested that talin dimer formation only occurs at higher protein concentrations (≥0.7 mg/ml). Since, however, for both rotary shadowing and analytical ultracentrifugation, relatively low protein concentrations were used, i.e., between 0.1 and 0.4 mg/ml, we do not believe that the observed dimer species is simply the result of a concentration-dependent monomer–dimer equilibrium, particularly since we have not observed any significant amounts of monomer under any conditions tried.

Using glutaraldehyde as a covalent cross-linking agent, we have been able to stabilize talin in its dimer configuration, which was the only oligomeric state observed by SDS–PAGE (see Fig. 4A). The ability of talin to nucleate actin filament formation should lead to an increase of filament number concentration which, as observed, should give rise to an increase of the fluorescence signal of NBD-labeled actin (see Fig. 5) and a reduction of the low-shear viscosity (Fig. 5, inset) in rheological assays (Kaufmann *et al.*, 1991; Goldmann *et al.*, 1992; Ruddies *et al.*, 1993). We have presented convincing evidence that the nucleating activity is almost fully retained when using GA-cross-linked talin dimers instead of unmodified talin. Importantly, however,

these nucleating effects of both native and cross-linked talin are only observed during the early time course of polymerization (≤10 min). This is because over time the shorter actin filaments formed in the presence of talin anneal to form a highly viscous actin network (Ruddies *et al.*, 1993). The failure to depict any significant reduction of actin filament length in the presence of talin as reported by Schmidt *et al.* (1993) must be due to the 5-min pre-incubation of talin with actin followed by a further >15-min incubation of the polymerization mixture at 25°C, which is beyond the time required for EM studies to demonstrate a reduction of actin filament length in the minute range (≤10 min; see Fig. 2). These data are fully consistent with our previously published light microscopic measurements of actin filament length reduction by talin over short periods of time (Kaufmann *et al.*, 1992).

All data considered, we have to conclude that in its functional state, talin, very much like α-actinin, spectrin, and dystrophin (Cross *et al.*, 1990; Dhermy, 1991), is a dumbbell-shaped antiparallel homodimer. This dimer configuration may not only be required for talin to interact with actin but also for its observed binding to vinculin (Gilmore *et al.*, 1993), integrin (Horwitz *et al.*, 1986), and possibly to membranes.

The authors are grateful to Ariel Lustig (Biocenter, University, Basel) for performing the analytical ultracentrifugation, to Dr Stefan Kaufmann for carrying out polymerization assays, and to Ms. H. Kirpal for protein preparations. This work was supported by grants from Deutsche Forschungsgemeinschaft (DFG Is 25/7-1 and SFB 266/C5 to G.I.), the Swiss National Science Foundation (31-30129.90 to U.A.), and the M. E. Müller Foundation of Switzerland. A.B. is the recipient of a postdoctoral fellowship from the Human Frontier Science Program Organization. This work was presented as a poster at the ASCB Meeting in New Orleans 1993 and published in *Molecular Biology of the Cell* (1993) Suppl. 4, p. 150a in abstract form.

REFERENCES

Aebi, U., and Pollard, T. (1987) A glow discharge unit to render electron microscope grids and other surfaces hydrophilic. *J. Electron Microsc. Tech.* 7, 29–33.

Bevington, P. R. (1969) Data Reduction and Error Analysis for the Physical Sciences, pp. 204–246, McGraw–Hill, New York.

Bradford, M. (1976) A rapid and sensitive method for the quantitation of μg quantities of protein utilizing the principle of protein-dye binding. *Anal. Biochem.* 72, 248–254.

Burridge, K., and Connell, L. (1983) A new protein of adhesion plaques and ruffling membranes. *J. Cell Biol.* 97, 359–367.

Chernyak, V. Y., and Magretova, N. N. (1982) An "all-speed" autocalibration method for sedimentation equilibrium in dilute homogeneous and multicomponent solutions. *Anal. Biochem.* 123, 101–109.

Cross, R. A., Stewart, M., and Kendrick-Jones, J. (1990) Structural predictions for the central rod domain of dystrophin. *FEBS Lett.* 262, 87–92.

DePasquale, J. A., and Izzard, C. S. (1991) Accumulation of talin in nodes at the edge of lamellipodium and separate incorporation into adhesion plaques at focal contacts in fibroblasts. *J. Cell Biol.* 113, 1351–1359.

Dhermy, D. (1991) The spectrin Super-family. *Biol. Cell.* 71, 249–254.

Dietrich, C., Goldmann, W. H., Sackmann, E., and Isenberg, G. (1993) Interaction of NBD-talin with lipid monolayers: A film balance study. *FEBS Lett.* 324, 37–40.

Fowler, W., and Aebi, U. (1983) Preparation of single molecules and supra-molecular complexes for high resolution metal shadowing. *J. Ultrastruct. Res.* 83, 319–334.

Gilmore, A. P., Wood, C., Ohanian, V., Jackson, P., Patel, B., Rees, D. J. G., Hynes, R. O., and Critchley, D. R. (1993) The cytoskeletal protein talin contains at least two distinct vinculin binding domains. *J. Cell Biol.* 122, 337–347.

Goldmann, W. H., and Isenberg, G. (1991) Kinetic determination of talin-actin binding. *Biochem. Biophys. Res. Commun.* 178, 718–723.

Goldmann, W. H., Niggli, V., Kaufmann, S., and Isenberg, G. (1992) Probing actin and liposome interaction of talin and talin–vinculin complexes: A kinetic, thermodynamic and lipid labeling study. *Biochemistry* 31, 7665–7671.

Heise, H., Bayerl, T., Isenberg, G., and Sackmann, E. (1991) Human platelet P-235, a talin like actin binding protein, binds selectively to mixed lipid bilayers. *Biochim. Biophys. Acta* 1061, 121–131.

Horwitz, A., Duggan, K., Buck, C., Beckerle, M. C., and Burridge, K. (1986) Interaction of plasma membrane fibronectin receptor with talin—A transmembrane linkage. *Nature (London)* 320, 531–533.

Isenberg, G. (1991) Actin binding proteins-lipid interactions. *J. Muscle Res. Cell Motil.* 12, 136–144.

Isenberg, G., and Goldmann, W. H. (1992) Actin-membrane coupling: A role for talin. *J. Muscle Res. Cell Motil.* 13, 587–589.

Isenberg, G., and Goldmann, W. H. (1994) Actin binding proteins–lipid interactions, in Hesketh, J. E. & Pryme, I. F. (eds.), The Cytoskeleton. Vol. I. JAI Press, Greenwich. (In press.)

Isenberg, G., Small, J. V., and Kreutzberg, G. W. (1978) Correlation between actin polymerization and surface receptor seggregation in neuroblastoma cells treated with concanavalin A. *J. Neurocytol.* 7, 649–661.

Kaufmann, S., Piekenbrock, T., Goldmann, W. H. Bärmann, M., and Isenberg, G. (1991) Talin binds to actin and promotes filament nucleation. *FEBS Lett.* 284, 187–191.

Kaufmann, S., Käs, J., Goldmann, W. H., Sackmann, E., and Isenberg, G. (1992) Talin anchors and nucleates actin filaments at lipid membranes: A direct demonstration. *FEBS Lett.* 314, 203–205.

Laemmli, U. K. (1970) Cleavage of structural proteins during the assembly of the head of bacteriophage T4. *Nature (London)* 227, 680–685.

MacLean-Fletcher, S. D., and Pollard, T. D. (1980) Identification of a factor in conventional muscle actin preparations which inhibits actin filament self-association. *Biochem. Biophys. Res. Commun.* 96, 18–27.

McLachlan, A. D., Stewart, M., Hynes, R. O., and Rees, J. G. D. (1994) Analysis of repeated motifs in the talin rod. *J. Mol. Biol.* 235, 1278–1290.

Millonig, R., Salvo, H., and Aebi, U. (1988) Probing actin polymerization by intermolecular cross-linking. *J. Cell Biol.* 106, 785–796.

Molony, L., McCaslin, D., Abernethy, J., Paschal, B., and Burridge, K. (1987) Properties of talin from chicken gizzard smooth muscle. *J. Biol. Chem.* 262, 7790–7795.

Muguruma, M., Matsumura, S., and Fukazawa, T. (1990) Direct

interactions between talin and actin. *Biochem. Biophys. Res. Commun.* **171**, 1217–1223.

Niggli, V., Kaufmann, S., Goldmann, W. H., and Isenberg, G. (1994) Identification of functional domains in the cytoskeletal protein talin. Submitted for publication.

Rees, D. J. G., Ades, S. E., Singer, S. J., and Hynes, R. O. (1990) Sequence and domain structure of talin. *Nature (London)* **247**, 685–689.

Ruddies, R., Goldmann, W. H., Isenberg, G., and Sackmann, E. (1993) The viscoelasticity of entangled actin networks: The influence of defects and modulation by talin and vinculin. *Eur. Biophys. J.* **22**, 309–321.

Schmidt, J. M., Robson, R. M., Zhang, J., and Stromer, M. H. (1993) The marked pH dependence of the talin–actin interactions. *Biochem. Biophys. Res. Commun.* **197**, 660–666.

Small, J. V., Isenberg, G., and Celis, J. E. (1978) Polarity of actin at the leading edge of cultured cells. *Nature (London)* **272**, 638–639.

Spudich, J. A., and Watts, S. (1971) The regulation of rabbit skeletal muscle concentration. *J. Biol. Chem.* **246**, 4866–4871.

Wrigley, N. G. (1968) The lattice spacing of crystalline catalase as an internal standard of length in electron microscope. *J. Ultrastruct. Res.* **24**, 454–464.